Co-substrate utilisation in “Candidatus Accumulibacter” enhances metabolic fitness in dynamic environments

Páez-Watson, Timothy; Jansens, Casper; van Loosdrecht, Mark C.M.; Roy, Samarpita

DOI
10.1016/j.watres.2025.124401

Publication date
2025

Document Version
Final published version

Published in
Water Research

Citation (APA)
Páez-Watson, T., Jansens, C., van Loosdrecht, M. C. M., & Roy, S. (2025). Co-substrate utilisation in “Candidatus Accumulibacter” enhances metabolic fitness in dynamic environments. *Water Research*, *287*, Article 124401. https://doi.org/10.1016/j.watres.2025.124401

Water Research 287 (2025) 124401

Contents lists available at ScienceDirect

Water Research

journal homepage: www.elsevier.com/locate/watres

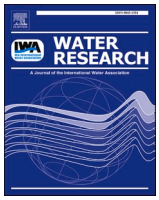

Co-substrate utilisation in "*Candidatus* Accumulibacter" enhances metabolic fitness in dynamic environments

Timothy Páez-Watson, Casper Jansens, Mark C.M. van Loosdrecht, Samarpita Roy *

Delft University of Technology, Department of Biotechnology, Delft, the Netherlands

ARTICLE INFO

Keywords:
Co-substrate metabolism
Candidatus Accumulibacter
Synergistic interactions
Microbial ecophysiology
Metabolic optimality

ABSTRACT

Optimizing resource use is essential for the survival and fitness of species in microbial communities ubiquitous in natural and engineered ecosystems. These ecosystems are often characterized by the simultaneous presence of multiple substrates such as volatile fatty acids, amino acids and sugars. Yet, the evaluation of metabolic potential for these microbial community members is predominantly based on single substrate utilisation. Metabolic and ecological implications of the interactions of multiple substrates, particularly in environments with changes in redox conditions and substrate availability, remain poorly understood. In this study, we investigate the metabolic interactions resulting from co-substrate utilization in polyphosphate-accumulating organisms within wastewater treatment systems. We combined experimental analysis of highly enriched "*Ca.* Accumulibacter" mixed cultures with genome-resolved metagenomics and conditional flux balance analysis (cFBA) to quantify the physiological relevance of co-substrate uptake. We observe that anaerobic co-substrate utilisation of acetate and aspartate result in metabolic interactions leading to optimized redox balance, reduced ATP losses and increased biomass yields by up to 8% compared to individual substrate use. Metabolic modelling revealed that these benefits emerge from the network topology, where the interaction of different metabolic routes gives rise to synergistic effects. Extending our analysis to additional substrate pairs, we classify metabolic interactions into three general types: (i) neutral, (ii) one-way synergistic and (iii) reciprocal synergistic. Our findings highlight the importance of metabolic interactions and cellular resource allocation strategies in dynamic microbial ecosystems. This study provides a broader ecological framework for understanding competitive metabolic strategies in environmental organisms. Co-substrate utilization can have direct implications for improving the yield or productivity of bioprocesses.

1. Introduction

Environments containing only a single substrate are rare in nature, and wastewater treatment plants, which harbour natural mixed microbial communities, are no exception. Wastewater typically contains a mixture of organic substrates, including fatty acids, amino acids, sugars and lipids (Huang et al., 2010, Bengtsson et al., 2008, Qiu et al., 2019, Carvalheira et al., 2014). Polyphosphate Accumulating Organisms (PAOs) are keystone species performing Enhanced Biological Phosphorous Removal (EBPR) in wastewater treatment plants. EBPR systems are complex, dynamic environments dominated by members of the genus "*Ca.* Accumulibacter", both in terms of biovolume (Lu et al., 2006, Páez-Watson et al., 2024) and protein content (Kleikamp et al., 2022, Kleikamp et al., 2023), highlighting their key role in the biological conversions that drive this process. Their unique metabolic capabilities allow them to accumulate large amounts of polyphosphate (PolyP) (Mino et al., 1987, Kortstee et al., 1994) under cyclic, dynamic environments. Understanding co-substrate utilisation in "*Ca.* Accumulibacter" and other PAOs is therefore crucial for optimizing EBPR processes.

The metabolism of "*Ca.* Accumulibacter" depends on the cycling of polyhydroxyalkanoates (PHAs), PolyP and glycogen during an EBPR cycle (Smolders et al., 1994, Smolders et al., 1994, Smolders et al., 1995). This enables the rapid anaerobic uptake and accumulation of volatile fatty acids (VFAs) inside the microbial cells. The stored polymers can be subsequently oxidized aerobically, generating enough energy for growth and the accumulation of PolyP. Despite their high prevalence in WWTPs, no pure cultures of "*Ca.* Accumulibacter" are available, making research reliant on highly enriched cultures (> 90 % biovolume (Lu et al., 2006, Páez-Watson et al., 2024)) for

* Corresponding author.
E-mail address: samarpita.roy@tudelft.nl (S. Roy).

https://doi.org/10.1016/j.watres.2025.124401
Received 16 May 2025; Received in revised form 9 July 2025; Accepted 12 August 2025
Available online 12 August 2025

characterization .

Research on this metabolic strategy has predominantly focused on feeding single substrates, such as VFAs like acetate (Van Loosdrecht et al., 1997, Mino et al., 1998, Welles et al., 2015) and propionate (Pijuan et al., 2004), as well as non-VFA substrates like glucose (Elahinik et al., 2023, Ziliani et al., 2023), and amino acids like aspartate and glutamate (Qiu et al., 2019). Despite the importance of mixed substrate in wastewater, studies on the metabolic mechanisms of "*Ca.* Accumulibacter" during the simultaneous uptake of two or more substrates are very limited. Studies have reported co-consumption of acetate with glucose (Ziliani et al., 2023, Gebremariam et al., 2012), acetate with propionate and lactate (Rubio-Rincón et al., 2019) and acetate with glycerol (Yuan et al., 2010) in enrichment cultures, but the interactions between the metabolic strategies for consumption of each substrate remains poorly understood. For example, Carvalheira et al. (2014) experimentally explored acetate and propionate co-feeding and demonstrated substrate competition effects, though without investigating synergistic or emergent interactions in detail (Carvalheira et al., 2014).

A notable study by Qiu et al. (Ziliani et al., 2023) stands out for its detailed examination of the concurrent uptake of acetate with either aspartate or glutamate. This research identified a potential synergy between acetate and aspartate, where aspartate uptake led to a net energy gain (~9 % ATP gain), enhancing acetate uptake. The proposed mechanism was the operation of fumarate reductase (reducing fumarate to succinate) which contributes to the *proton motive force* (pmf) required for acetate transport. More recently, a similar energetic gain was evaluated for acetate and succinate co-consumption (Chen et al., 2023), though the metabolic entry point of succinate bypasses fumarate reductase, raising the question of whether this synergy is indeed driven by *pmf* or a hitherto unidentified metabolic interaction. It is thus of particular interest to further examine the metabolic interactions underlying the concurrent uptake of acetate and aspartate, given their distinct metabolic entry points, relevance in wastewater environments, and the previously observed energetic synergy.

Understanding the interactions within metabolic networks is challenging due to the complexity and interconnectedness of metabolites, especially energy carriers like ATP, NADH, $FADH_2$ (Nielsen, 2017). In this regard, metabolic modelling provides valuable tools for studying these networks and how interactions emerge from stoichiometric rules. Techniques such as Flux Balance Analysis (FBA) can model steady-state metabolic operations (Orth et al., 2010), but more advanced methods are needed for dynamic systems like EBPR (Mahadevan et al., 2002, Sarkar et al., 2019, Liu and Bockmayr, 2020). One such method is conditional FBA (cFBA) (Rügen et al., 2015), which has been successfully used to model "*Ca.* Accumulibacter" metabolism, where intracellular storage polymers cycling emerged as a property of model stoichiometry and environmental conditions (Páez-Watson et al., 2023). However, how these emergent properties change with co-substrate utilisation remains an open question. We hypothesize that co-substrate utilization in "*Ca.* Accumulibacter" will lead to metabolic interactions affecting the redox balance and potentially alter the type and level of intracellular storage polymer usage. Answering these questions can enhance the design and operation of bioprocesses that utilize waste streams with diverse organic carbon sources.

To address this, we aimed to understand the metabolic implications of co-substrate utilisation in "*Ca.* Accumulibacter" under the fluctuating environmental conditions characteristic of EBPR. We developed and tested a metabolic model for the uptake of varying ratios of acetate and aspartate to uncover synergistic interactions that improve growth yields. These findings were validated with lab-scale enrichments and the mechanisms behind the synergy are described. Finally, we extended this modelling approach to explore metabolic interactions of acetate with other co-substrates, identifying a basic biological principle of metabolic interactions. This work lays the groundwork for further exploration of co- substrate utilisation, which could potentially lead to increased biomass yields compared to individual substrate utilisation.

2. Materials and methods

2.1. "Ca accumulibacter" enrichment

A "*Ca.* Accumulibacter" enrichment was obtained in a 1.5 L (1 L working volume) sequencing batch reactor (SBR), following conditions described earlier (Páez-Watson et al., 2024) with some adaptations. The reactor was inoculated using enriched sludge from the work of Páez-Watson et al. (Páez-Watson et al., 2024), which was previously inoculated with activated sludge from a municipal wastewater treatment plant (Harnaschpolder, The Netherlands). Each SBR cycle lasted 6 h, consisting of 30 min of settling, 50 min of effluent removal, 10 min of N_2 sparging, 30 min of anaerobic feeding, 105 min of anaerobic phase and 135 min of aerobic phase. N_2 gas and compressed air were sparged at 500 ml/min into the reactor broth to maintain anaerobic and aerobic conditions respectively. The hydraulic retention time (HRT) was 12 h (removal of 500 mL of broth per cycle, each cycle of 6 h). The average solids retention time (SRT) was controlled to 9 days by the removal of 27,7 ml of mixed broth at the end of the mixed aerobic phase in each cycle. The pH was controlled at 7.3 ± 0.1 by dosing 0.5 M HCl or 0.5 M NaOH. The temperature was maintained at 20 ± 1 °C.

The reactor was fed with three separate media components diluted in demineralized water: a concentrated COD medium (400 mg COD/L) of acetate (13 g/L sodium acetate × $3H_2O$); a concentrated mineral medium (0.69 g/L NH_4Cl, 2.16 g/L $MgSO_4 \times 7H_2O$, 0.54 g/L $CaCl_2 \times 2H_2O$, 0.64 KCl, 0.06 g/L N-allylthiourea (ATU), 0.06 g/L yeast extract and 6 mL/L of trace element solution prepared following Smolders et al. (Smolders et al., 1994); and a phosphate solution containing 0.76 g/L $NaH_2PO_4 \times H_2O$ and 0.8 g/L $Na_2HPO_4 \times 2H_2O$. In each cycle, 75 mL of COD medium, 75 ml of mineral medium and 360 mL of phosphate solution were added to the reactor during the 30 min of feeding. The final feed contained 400 mg COD/L of acetate.

2.2. Batch tests

Batch tests were conducted in the bioreactor on the enriched biomass once a *pseudo* steady state was reached (determined by a constant phosphate release and removal over multiple days). For the batch tests, 400 ml of H_2O and 50 ml of mineral media were fed as usual during the anaerobic phase. Later, 50 ml of organic substrate (containing either acetate, aspartate or a mix) was pulse fed and considered the beginning of the anaerobic phase of the cycle. The anaerobic phase on these batch tests was extended by 30 min to compensate for the delay in feed. The organic media was prepared such that the final feed contained 400 mg COD/L of acetate, aspartate or a mix (calculated by using the degree of reduction of 8 and 12 e^-/mol for acetate and aspartate, respectively). Thus, the organic substrate solution for the tests contained only acetate, only aspartate or mix of acetate and aspartate as follows: (i) 13.1 g/L sodium acetate trihydrate ($C_2H_3NaO_2 \cdot 3H_2O$), (ii) 19.35 g/L sodium aspartate ($C_4H_6NNaO_4$), or (iii) 5,8 g/L sodium acetate trihydrate with 9,6 g/L sodium aspartate. For mixed substrates, the net utilisation of acetate and aspartate was used to determine the acetate:aspartate uptake ratio.

2.3. Reactor and biomass analyses

Extracellular concentrations of phosphate and ammonium were measured with a Gallery Discrete Analyzer (Thermo Fisher Scientific, Waltham, MA). Acetate was measured by high performance liquid chromatography (HPLC) with an Aminex HPX-87H column (Bio-Rad, Hercules, *CA*), coupled to RI and UV detectors (Waters, Milford, MA), using 0.0015 M phosphoric acid as eluent supplied at a flowrate of 1 mL/min.

The biomass concentration (total and volatile suspended solids – TSS

and VSS) was measured in accordance with Standard Methods as described in Smolders et al. (Smolders et al., 1994) with some modifications: 10 ml of mixed broth were obtained at the end of the aerobic phase, centrifuged at 3600*g during 3 min and washed twice with demineralized water to remove salts. The sludge was then dried at 100 °C for 24 h and weighed on a microbalance to determine the dry content – TSS. The ash content was determined by incinerating the dry material in an oven at 550 °C, and the difference used to calculate the VSS.

For glycogen and PHA determination, biomass samples (10 ml mixed broth) were collected throughout the batch test and stored in 15 ml conical tubes containing 0.3 ml of 37 % formaldehyde to stop biological activity. After each batch test, the biomass tubes were pottered to break the granular structure of the biomass, centrifuged at 3700 *g for 5 min and washed twice. The pellet was then frozen at −80 °C for at least 3 h and freeze dried. For glycogen analysis the method described by Smolders et al. (Smolders et al., 1994) was used: 5 mg of dry biomass was digested in 0.9 M HCl solutions in glass tubes at 100 °C for 5 h. After this time, tubes were cooled at room temperature, filtered with 0.45 μm Whatman disk filters and neutralized with equal volumes of 0.9 M NaOH. The glucose resulting from digestion was quantified using the d-Glucose Assay Kit (GOPOD Format) from Megazyme (Bray, Ireland).

PHA extraction, approximately 30 mg of freeze-dried biomass was placed in a tube with 1.5 mL of 10 % sulfuric acid in methanol and 1.5 mL of chloroform. To each tube, 100 μL of an internal standard solution (0.01 g/mL benzoic acid in methanol) was added. The samples were then hydrolyzed and esterified at 100 °C for 5 h with periodic manual vortexing. Following this, 3 mL of ultrapure water was added to facilitate phase separation. The organic phase containing the esters was filtered and analyzed using a gas chromatograph (GC 6890 N, Agilent, USA). Quantifications of PHB, PH2MV, and PHV were performed using commercial standards, including 3-hydroxybutyrate, 2-hydroxyhexanoate, and a synthetic copolymer of (*R*)-3-hydroxybutyrate-(*R*)-3-hydroxyvalerate (Sigma-Aldrich, USA).

2.4. Metabolic model and cFBA simulations

The metabolism of "*Ca.* Accumulibacter" was simulated with cFBA using the py_cFBA toolkit implementation (Páez-Watson et al., 2024). A basic metabolic model was constructed as a stoichiometric matrix (**S**), representing the relationships between metabolites and reactions. Stoichiometries for reactions involved in glycogen degradation, glycolysis, the TCA cycle, anaplerotic routes, and PHA synthesis were adapted from an earlier study on "*Ca.* Accumulibacter" (Páez-Watson et al., 2024) in which the reactions were built based on available high quality MAGs. For this study, the reaction malate decarboxylase (catalysed by the malic enzyme *MalE)* was excluded from the metabolic model since it is only present in a few genomes within this genus. Stoichiometries for aspartate metabolism were obtained from Qiu et al. (Qiu et al., 2019) and the presence of this pathway in our enrichment culture was confirmed with metagenomics (see later in this section). A reaction representing synthesis of 1 c-mole of biomass was implemented in **S** following the stoichiometry from Loosdrecht et al. (Páez-Watson et al., 2023), which combined the energy (ATP) requirements for bacterial growth from acetyl-CoA from Gommers et al. (Gommers et al., 1988) and the overall stoichiometry of PAOs growth from Smolders et al. (Smolders et al., 1994, Oehmen et al., 2007).

In the model, selected metabolites were defined as imbalanced, allowing their accumulation or depletion over time during simulations. These included acetate, aspartate, glycogen, PHB, PH2MV, CO_2, polyP, and biomass. All other metabolites were balanced, adhering to the steady-state assumption of FBA. Biomass was defined as the sole contributor to the weights vector (w) in the cFBA formulation. The **S** matrix, together with details on imbalanced metabolites and the weights vector, is provided in the supplementary materials.

The model was implemented in Python using the py_cFBA toolkit, which generated SBML files for each configuration. Simulations of an EBPR cycle consisted of five time points ($\Delta t = 1$ hour), with no enzyme capacity constraints since this research is not centred on proteome constraints. Additionally, enzyme capacity constraints require accurate estimation of kinetic parameters for each metabolic enzyme which, for microbial communities, is limited.

Anaerobic and aerobic phases were simulated by allowing the reactions ETC_NADH, ETC_FADH (electron transport chain oxygen consumption), and biomass synthesis to occur exclusively in the final two time points of each cycle by setting the reaction upper bounds at 0 for the first 3 time points of the simulation. Reaction reversibility was defined using upper and lower bounds based on a prior thermodynamic evaluation (Páez-Watson et al., 2024) (see supplementary information S. M. 1 for each reaction definition).

Substrate uptake during the anaerobic phase was enforced using quota definitions. An equality-quota at the initial time point specified the concentration of substrate fed, followed by a max-quota of zero in subsequent time points. Substrate concentrations were normalized to provide equivalent degree of reduction (electron equivalents), even for substrate mixtures, based on their individual degree of reduction (*e.g.*, 8 electrons for acetate, 12 electrons for aspartate). All simulations optimized biomass synthesis as the global target across the entire cycle, rather than at each time step, consistent with cFBA methodology. Although the model does not rely on kinetic parameters or fitting, it produces quantitative predictions (glycogen, polyphosphate and PHAs yields) that were directly compared to experimental results. All SBML models, simulation files and results are available at https://github.com/TP-Watson/PAOs_co-substrates_cFBA.

2.5. Microbial community characterization

The microbial community of the reactor was characterized at pseudo steady state as defined earlier. Two orthogonal approaches were used for the community characterization: metagenomics and Fluorescence in-situ hybridization (FISH).

For FISH, samples underwent handling, fixation, and staining procedures outlined by Winkler et al. (Winkler et al., 2011). Bacteria were selectively identified using a blend of EUB338, EUB338-II, and EUB338-III probes labelled with cy5 (Amann et al., 1990, Daims et al., 1999). "*Ca.* Accumulibacter" was visualized employing a mixture of Acc1011, Acc471, Acc471_2, Acc635, Acc470 probes labelled with cy3 designed and tested previously for different "*Ca.* Accumulibacter" lineages (Petriglieri et al., 2022). *Dechloromonas* related PAOs were visualized employing a mixture of the Dech443 and Bet135 probes labelled with FLUOS together with Dech443c1 unlabelled competitive probe (Petriglieri et al., 2021, McIlroy et al., 2016). The images were captured with an epifluorescence microscope equipped with filter set Cy3 (ET545/25x ET605/70 m T565LPXR), Cy5 (ET640/30x ET690/50 m T660LPXR), and FITC (ET470/40x ET525/50 m T495LPXR) (Axio Imager M2, Zeiss, Germany). Quantitative FISH (qFISH) was done as a percentage of total biovolume over 12 representative pictures using the Daime software (DOME, Vienna, Austria) (Daims et al., 2006).

For metagenomics, DNA from the biomass samples was extracted using the DNeasy PowerSoil Pro-Kit (Qiagen, Germany) following the manufacturer's protocol. Shotgun sequencing was performed by Hologenomix (Delft, Netherlands). Paired-end sequencing with a read length of 150 bp was conducted using the Illumina NovaSeq X sequencing system. Library preparation was carried out using the Nextera XT DNA Library Preparation Kit. Approximately 10 Gbp of sequencing data were generated per sample.

The quality of raw sequenced reads was assessed using FastQC (version 0.11.7) with default parameters (Andrews, 2010), and results were visualized with MultiQC (version 1.19). Low-quality paired-end reads were trimmed and filtered using Fastp (version 0.23.4) in paired-end mode (Chen, 2023). Taxonomic classification of raw reads was performed to profile the microbiome in each sample using Kraken2 (version 2) with the standard database, which includes all complete

bacterial, archaeal, and viral genomes in the NCBI RefSeq database, complemented by a curated wastewater database (sludgeDB) (Wood et al., 2019).

Clean reads were assembled into contigs using MetaSPAdes (version 3.15.5) with default parameters (Nurk et al., 2017). The resulting contigs were binned using MetaBAT (version 2.2.15) to reconstruct metagenome-assembled genomes (MAGs) with default parameters (Kang et al., 2019). Bin completeness and contamination were assessed using CheckM (version 1.2.2) with the "lineage_wf" workflow (Parks et al., 2015). A cut-off of ≥90 % completeness and ≤5 % contamination was applied for bin selection. Relative abundance of bins with contamination below 5 % was determined in each sample using CoverM (version 0.7.0, https://github.com/wwood/CoverM) with default parameters.

For phylogenetic analysis, bins were classified using GTDB-Tk (version 2.4.0) and GTDB release 220 (Chaumeil et al., 2022). The *ppk1* gene was utilised as a marker in bins identified as Accumulibacter. hmmsearch (Johnson et al., 2010) was used with the ppk1.hmm profile, taking the best hit as the *ppk1* gene. Identified *ppk1* genes were combined with those in an existing database and aligned with MUSCLE (version 5.1) (Edgar, 2004). A phylogenetic tree of these *ppk1* sequences was generated with RaxML-NG (version 1.2.2) (Kozlov et al., 2019) and visualised using iTol (v6) (Letunic and Bork, 2024). Sequencing data was deposited under the BioProject no. PRJNA1191880, BioSample accession no. SAMN45106973.

3. Results

3.1. Different anaerobic phenotypes are employed for acetate, aspartate and combined substrate uptake by "Ca. Accumulibacter"

We expanded a previous metabolic model of "*Ca.* Accumulibacter" (Páez-Watson et al., 2024) to incorporate uptake mechanisms for acetate and aspartate (Fig. 1A). Next, we simulated the concurrent uptake of both substrates at varying ratios. To normalize the simulations, we ensured that both substrates combined provided the same amount of electron equivalents (analogous to the chemical oxygen demand, most widely used in engineering), meaning the ratios were adjusted to achieve 'electron equivalence' rather than molar equivalence (see methods for details), since acetate and aspartate at equal molar concentrations would contribute unequally to the total electron (COD) load, leading to an imbalanced comparison of their metabolic impact.

The predictions indicated that the optimal anaerobic metabolic strategies for acetate or aspartate uptake were different, reflecting substrate-specific metabolic constraints. Moreover, when both substrates were utilised simultaneously, the resulting metabolic strategy was not a linear combination of the individual strategies, but rather an emergent reconfigured metabolic operation (Fig. 1B).

With acetate as the sole substrate, polyP and glycogen were degraded to supply resources for PHA accumulation primarily as acetyl-CoA precursors with a smaller fraction of propionyl-CoA. As the fraction of aspartate uptake increased, less glycogen degradation was required and larger fraction of PHAs as propionyl-CoA precursors was synthesized. At an equal electron equivalence ratio of acetate to aspartate, glycogen degradation halted. In scenarios with higher aspartate fractions, glycogen degradation was not observed, and the PHA pool showed a higher dominance of propionyl-CoA precursors with a higher demand for polyphosphate degradation (Fig. 1B).

To validate the modelling results, batch tests were performed on a lab reactor enrichment culture. qFISH analysis estimated the biovolume abundance of "*Ca.* Accumulibacter" at 89 ± 3 %., while metagenomics analysis revealed the enrichment of a clade I strain closely related to "*Ca.* Accumulibacter regalis". The enriched genome harboured the complete genetic potential required for aspartate metabolism (Fig. 2A).

Substrate compositions were evaluated in batch tests under three regimes: acetate, aspartate and a mix that resulted in a ratio of 45:55 electron equivalence acetate to aspartate uptake (regimes marked in Fig. 1B). The experimental results closely matched the predicted stoichiometries (Fig. 2B). Specifically, in the acetate-fed regime, PHAs accumulated anaerobically mainly as acetyl-CoA precursors,

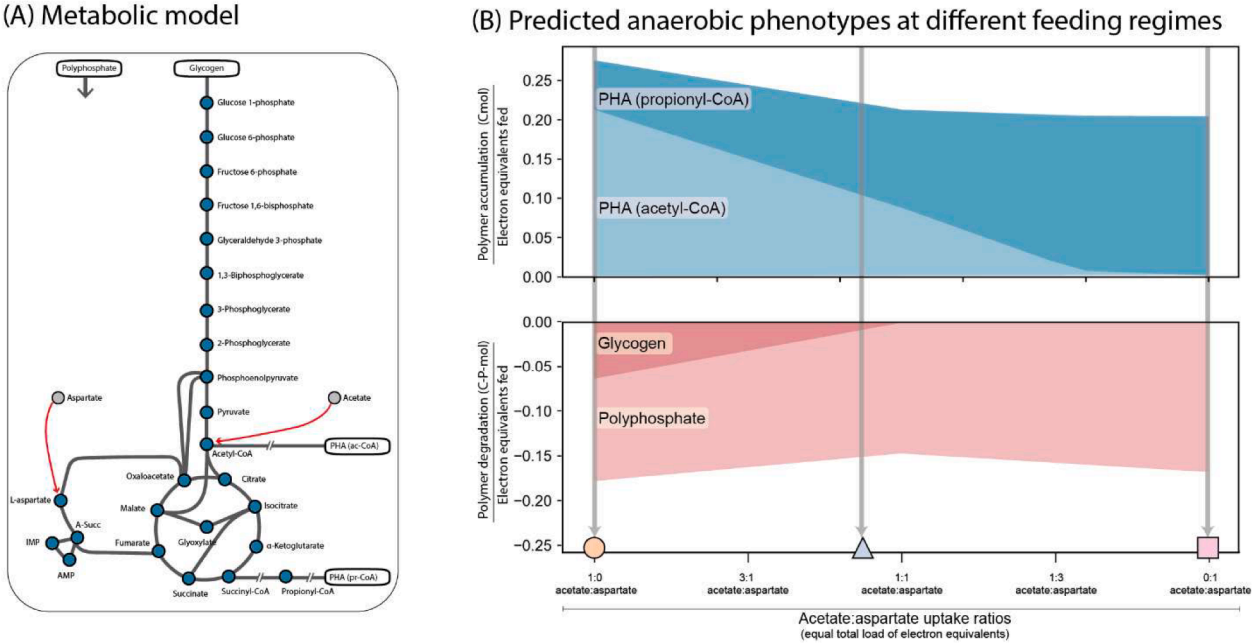

Fig. 1. Different anaerobic stoichiometries employed for the uptake of acetate, aspartate and combined substrates. **(A)** Schematic representation of the metabolic model of "*Ca.* Accumulibacter" used for simulations. Metabolites are represented as filled circles connected via reactions with grey lines. Red arrows indicate the entry point for substrate uptake in central carbon metabolism. Intracellular storage polymers are represented as white boxes. **(B)** Anaerobic conversions during the uptake of acetate/aspartate at varying electron equivalent ratios simulated with cFBA. (In blue) PHA accumulation subdivided into PHAs from acetyl-CoA (C2) and from propionyl-CoA (C3). (In red) Glycogen and Polyphosphate consumption. Three specific simulations marked with symbols (circle, triangle and square) were confirmed experimentally in Fig. 2.

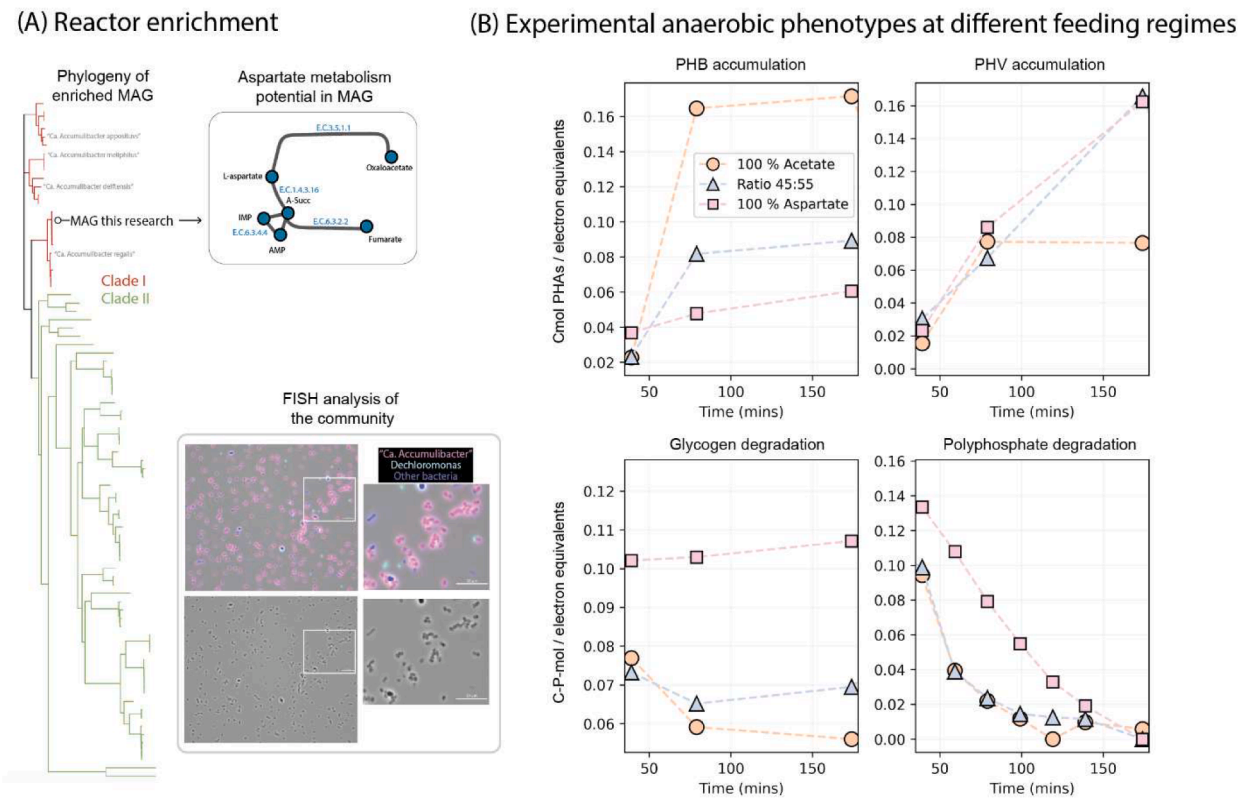

Fig. 2. Lab culture enrichment and experimental validation of the model. (A) Microbial community analysis with metagenomics and FISH. Metagenomics revealed the enrichment of an MAG closely associated to *Ca.* Accumulibacter Clade I "*Ca.* Accumulibacter regalis" and harbouring all the genes necessary for aspartate metabolism. FISH image of the enrichment in which magenta colour represents the overlap of "*Ca.* Accumulibacter" (red) and eubacteria (blue), cyan represents the overlap of Dechloromonas (green) and eubacteria (Supplementary Information S.M.3). Bottom image of phase contrast highlighting typical morphology observed from PAOs enrichments. **(B)** Experimental validation of the anaerobic phase metabolic strategies observed during batch tests for acetate, aspartate, and mixed acetate:aspartate (45:55 electron equivalence) regimes. Distinct markers (circles, triangles, and squares) facilitate direct comparison with the modelled predictions in Fig. 1.B.

accompanied by the degradation of polyphosphate and glycogen. In the mixed substrate regime, PHAs accumulated as a balanced mixture of both acetyl-CoA and propionyl-CoA precursors, with lower glycogen degradation per electron equivalent consumed compared to the acetate-only regime, consistent with the predictions. Finally, in the aspartate-fed regime, PHAs accumulated with a substantial decrease in acetyl-CoA precursors. This regime required the highest polyphosphate degradation and no glycogen degradation, aligning with the predictions (See Fig. 1B and Fig. 2B for comparison).

3.2. Metabolic and energetic balances reveal complementary strategies for the uptake of acetate and aspartate leading to enhanced growth yields

Simulations with varying ratios of acetate and aspartate in the feed revealed not only changes in internal storage polymer utilization under anaerobic conditions but also predicted maximum growth yields per electron equivalents for each cycle (Fig. 3A). Growth on aspartate was more efficient than growth on acetate. Notably, the highest growth yield was achieved with a combination of both substrates, specifically at a 1:4 electron equivalent ratio of acetate to aspartate.

During acetate uptake, glycogen was degraded to supply NADH necessary for PHA accumulation. The most efficient strategy for PHA accumulation reflected in the model involved glycogen degradation via glycolysis to phosphoenolpyruvate (PEP), then converting PEP to oxaloacetate (OAA) to fuel the TCA cycle. This allowed partial acetate oxidation in the right branch of the TCA cycle, producing NADH and Propionyl-CoA-type PHAs (Fig. 3B – region I). However, during the aerobic phase, this strategy required glycogen replenishment and the resulting glycolysis/gluconeogenesis operation over the cycle results in a net ATP loss, thus reducing the overall growth yield (Oehmen et al., 2007).

As the aspartate-to-acetate ratio increased, aspartate metabolism generated additional NADH via aspartate oxidase that countered the NADH requirement from glycogen degradation (Fig. 3B – region II), thus lowering the net ATP loss in the glycolysis/gluconeogenesis cycle, which improved growth yields. When the ratio reached 1:1, glycogen degradation was no longer necessary. Beyond this point, up to a 1:4 acetate-to-aspartate ratio, there were no net ATP losses, resulting in the highest growth yields (Fig. 3B – region III). In this range reciprocal benefits were observed when aspartate utilisation provided NADH that benefited acetate metabolism, while acetate utilisation supplied acetyl-CoA equivalents that supported aspartate metabolism (as described below).

At higher aspartate fractions, the metabolic strategy necessitated the operation of the right branch of the TCA cycle, which required acetyl-CoA equivalents. These equivalents could be supplied through acetate uptake. At insufficient acetate fractions, part of the consumed aspartate was channelled towards acetyl-CoA generation via PEP carboxykinase (PEPCK), raising the demand for ATP (Fig. 3B – region IV). This was met with an increased polyphosphate degradation, necessitating increased ATP requirements in the aerobic phase to replenish the polyphosphate pools resulting in lower growth yields.

3.3. Synergistic effects of co-substrate utilisation vary by metabolic entry point and network topology

Several substrates were incorporated into the existing metabolic model of "*Ca.* Accumulibacter", and their co-utilisation with acetate at varying ratios was simulated using cFBA, as described in the previous

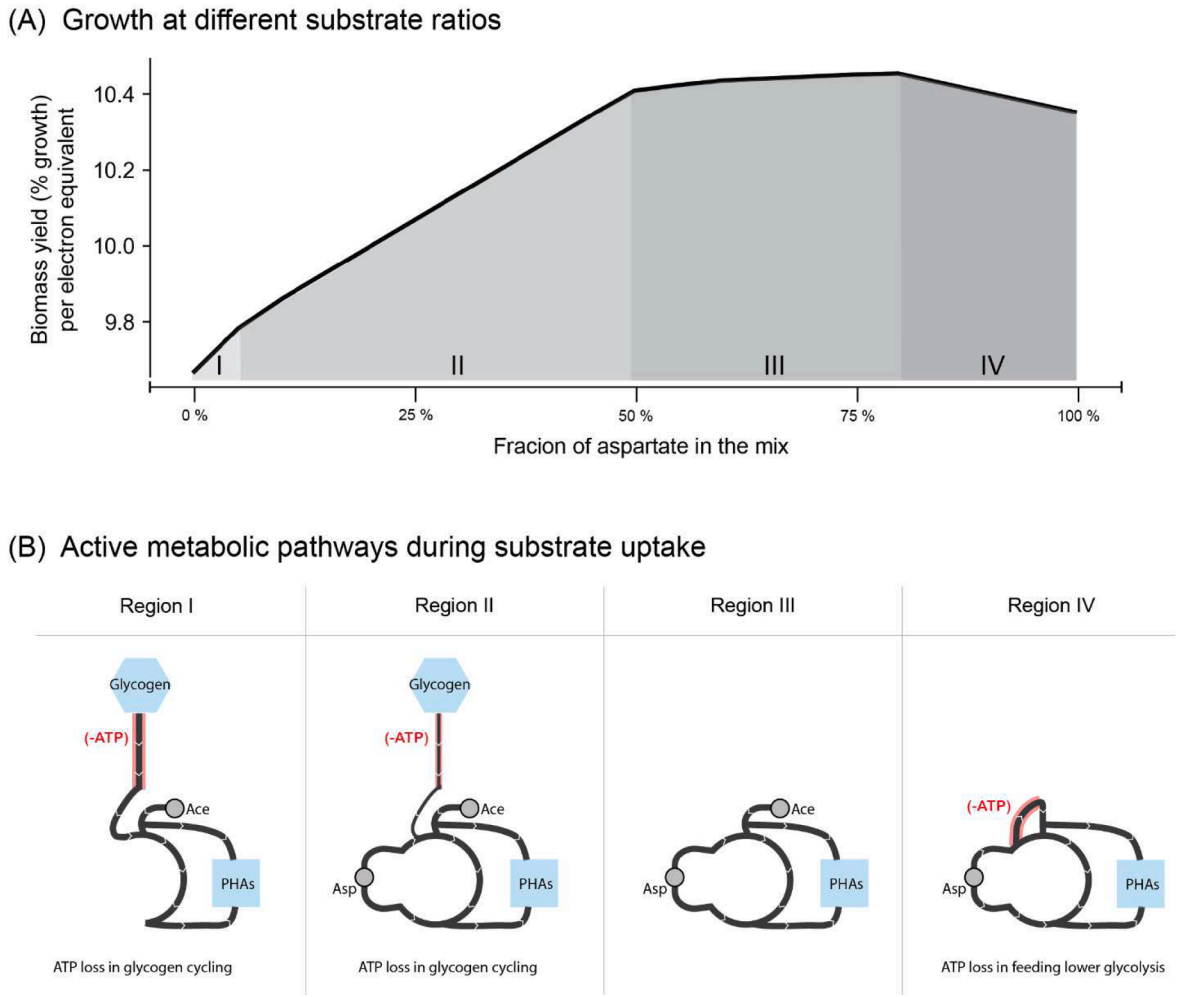

Fig. 3. (A) Biomass yield is expressed as the percent increase in biomass per EBPR cycle per electron equivalent of substrate fed. The x-axis indicates the fraction of aspartate based on electron equivalents (0 = pure acetate, 1 = pure aspartate). (B) Active metabolic operation during anaerobic substrate uptake predicted via the cFBA model at each region indicated in (A). Metabolic reactions contributing to a net ATP loss of the system considering the whole EBPR cycle have been highlighted in red. Lower thickness in Region II illustrates the lower demand on glycogen degradation than in Region I.

section. The predictions indicated that multiple substrates could support PHA accumulation without relying on reducing equivalents from glycogen degradation, which is typically required during anaerobic acetate uptake (Fig. 4).

Interestingly, the co-substrate utilisation of these substrates with acetate mirrored the reciprocal synergistic effect observed with aspartate. Specifically, these combinations led to an enhanced biomass yield per electron equivalent compared to the yield of individual substrates. We referred to these as reciprocal synergistic interactions. Along with acetate, co-substrates exhibiting this behaviour included succinate, fumarate, malate, oxaloacetate, and aspartate, all of which enter the reducing branch (left-hand side) of the TCA cycle. The co-substrate utilisation resulted in sufficient NADH production to alleviate the dependence from glycogen degradation, the main limitation during acetate uptake. Complementarily, metabolising these substrates benefited from the uptake of acetate to feed acetyl-CoA equivalents into the TCA cycle, as was the case with aspartate.

In contrast, another class of co-substrates when utilized with acetate produced biomass yields greater than the sum of the individual parts but did not surpass the yield of the more favourable substrate on its own. These substrates were able to generate sufficient reducing power (NADH) to alleviate the reliance on glycogen degradation, releasing the limitation for acetate metabolism. However, they did not benefit from the additional acetate uptake, since their metabolism did not require acetyl-CoA to be fed into the TCA cycle using PEPCK or similar reactions. We classified these as one-way synergistic interactions, observed for butyrate, lactate, pyruvate and citrate.

Finally, certain co-substrates such as propionate and alpha-ketoglutarate resulted in biomass yields that closely matched the sum of the individual yields, with no additional gain from co-utilisation. We classified these as neutral interactions, wherein the metabolic demands of these substrates closely resembled that of acetate. These substrates required similar resources (NADH and ATP) as acetate, leading to overlapping metabolic strategies that did not enhance overall growth yield.

To further explore the basis of the observed substrate synergies, we repeated the analysis after modifying the metabolic model to relax a few thermodynamic constraints (see Supplementary Materials S.M.2). Specifically, we removed the irreversibility of *PEPC* and *PEPCK* reactions, allowing them to operate as an internal cycle generating ATP – an outcome that is thermodynamically infeasible but useful for mechanistic exploration. Under these conditions, predicted biomass yields became flat across all substrate combinations (unlike the shapes from Fig. 3A and Fig. 4B) indicating no gains or losses in growth per electron equivalent fed. In other words, having an unlimited source of ATP breaks the synergy between substrate pairs, validating our findings that these interactions are driven by optimized ATP usage under physiological constraints.

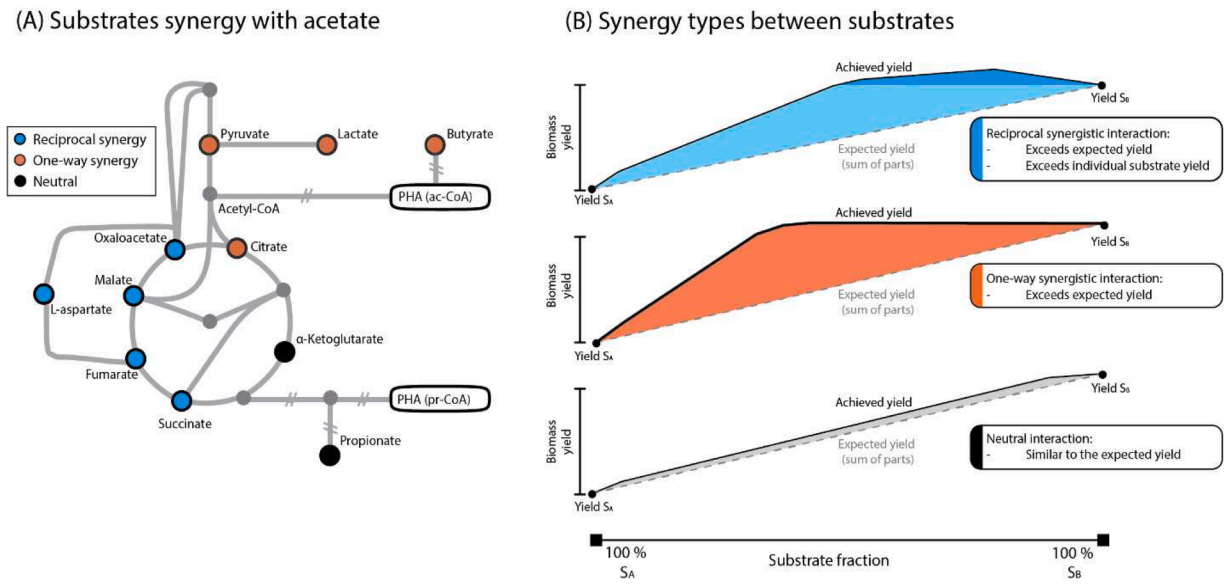

Fig. 4. Co-substrate interactions. **(A)** Metabolic model of "*Ca.* Accumulibacter" highlighting the external substrates that were tested and their type of interaction when co-fed with acetate. Blue: reciprocal synergistic interaction. Orange: one-way synergistic interaction. Black: neutral interaction. **(B)** Types of interactions (substrate synergy) existing between two substrates. Top shows reciprocal synergy between acetate and aspartate in which the biomass yield can exceed that of the sum of parts and the individual maximum biomass yields. Middle panel shows a one-way synergistic interaction between acetate and lactate in which the biomass yield can exceed that of the sum of parts but not the individual maximum yield. Bottom panel shows a neutral interaction between acetate and propionate in which the biomass yield is similar to the expected from the sum of parts.

4. Discussion

This study demonstrates that "*Ca.* Accumulibacter" exhibits synergistic metabolic interactions when co-utilising acetate and aspartate, leading to enhanced growth yields and reduced net ATP losses. These findings offer new insights into the broader ecological principles of microbial resource allocation and competition, where the ability to efficiently utilize diverse substrates can confer a selective advantage under fluctuating environments. The observed synergy highlights how co-substrate utilization can reshape metabolic strategies and is an emergent property dictated by network topology and metabolic interactions. Below, we contextualize these results within existing research on EBPR, biological adaptation, energy cycling, and implications for bioprocess design, while also acknowledging the limitations of the predictive models used.

Wastewater typically consists of a mix of organic substrates (Huang et al., 2010, Bengtsson et al., 2008, Qiu et al., 2019, Toja Ortega et al., 2021), and many studies have documented "*Ca.* Accumulibacter" as capable of consuming multiple substrates (Letunic and Bork, 2024), both through genomic analysis (Qiu et al., 2019, Oyserman et al., 2016) and *in situ* studies (Kong et al., 2004, Nguyen et al., 2015, Roy et al., 2021). In this study, we identified the enrichment of a clade I strain closely related to "Candidatus Accumulibacter regalis." However, genomic analyses suggest that key genes involved in aspartate utilization are also present in clade II members of Accumulibacter (IIA, IIF) (García Martín et al., 2006, Skennerton et al., 2015). Our findings align with these observations, showing that co-utilisation of acetate and aspartate not only is possible but also results in a metabolic interaction that optimizes cellular resource utilization pertaining to maximizing biomass yield. The reciprocal synergy observed arises from a two-way release of metabolic limitations for each substrate, improving overall biomass yield (Fig. 3). Specifically, acetate uptake is typically limited by anaerobic glycogen degradation, resulting in net ATP loss (Smolders et al., 1995, Sharma et al., 2024), while aspartate uptake requires ATP-consuming conversion of acetyl-CoA via PEPCK (Qiu et al., 2019). The combination of both substrates alleviates these limitations, leading to improved growth. It is noteworthy that the identified release in metabolic limitations were not dependent on potential *pmf* generation as hypothesized by Qiu et al. (Qiu et al., 2019) and thus can also explain the results obtained by Chen et al. (Chen et al., 2023) which contradicted the former *pmf* hypothesis. Our findings demonstrate clearly that these benefits are emergent network properties governed by energy flows and redox balance.

The energy losses associated with glycogen cycling during acetate utilisation in "*Ca.* Accumulibacter" has been well documented (Mino et al., 1987, Smolders et al., 1995, Van Loosdrecht et al., 1997, da Silva et al., 2020, Brdjanovic et al., 1998, Brdjanovic et al., 1998, Oehmen et al., 2010), but their direct impact on microbial fitness and growth efficiency has not been fully explored. Research manipulating growth rates by adjusting biomass retention time suggest that higher glycogen cycling corresponds to lower biomass yields (Rodrigo et al., 1999, Whang and Park, 2006, Onnis-Hayden et al., 2020), though the connection to energetics and metabolism has not been discussed extensively. Our results provide a mechanistic explanation by demonstrating how co-substrate utilisation can alleviate ATP losses. Our findings suggest that the energetic cost of glycogen cycling associated with acetate metabolism in "*Ca.* Accumulibacter" can be alleviated through co-substrate utilization (*e.g.* aspartate, butyrate, lactate, pyruvate, citrate, oxaloacetate, malate, fumarate and succinate; see Fig. 4). A similar advantage has been shown when microbial pure cultures co-utilize multiple carbon sources in carbon-limited chemostats, leading to greater substrate conversion efficiency and lower residual substrate concentrations (Egli et al., 1993), yet to our knowledge this is the first report of such effects in a complex dynamic ecosystem.

The energetic cost of glycogen cycling is comparable to "ATP demanding yet useful" cycles (Sharma et al., 2024), a broader biological phenomenon observed across microbial systems. However, since the ATP loss in cycling glycogen is temporally separated, this is not a futile cycle *sensu stricto*. Yet the temporal separation of glycogen degradation and replenishment serves an adaptive purpose, allowing organisms to maintain metabolic flexibility in response to dynamic environments. This flexibility supports survival and growth under fluctuating conditions, similarly as that of apparent ATP-demanding pathways (Chitraju et al., 2017, Sharma and Wolfrum, 2023, Zhang et al., 2016, Adolfsen and Brynildsen, 2015). Further consideration of the metabolic and

energetic cost/benefit of these temporally separated cycles needs to be considered, not only during wastewater treatment but more generally in organisms living in fluctuating condition such as oceans (Whitton, 2012, Reimers et al., 2017), soils (Wu et al., 2022), and many more dynamic environments (Wollmuth and Angert, 2023).

The interaction between the metabolic operations of acetate and aspartate is complex, due to the inherent complexity of metabolic networks (Liu et al., 2020) and the dynamic, cyclic nature of the EBPR cycle. The metabolic consequences of anaerobic uptake strategies can only be fully understood when considering the entire cycle. Most research in EBPR focuses on anaerobic processes, where the cell's redox state is tightly constrained, limiting reaction feasibility (Páez-Watson et al., 2024). However, without a holistic perspective on the aerobic phase, it is difficult to assess how anaerobic pathways impact overall metabolic fitness. The cFBA model employed here provides a tool to explore these interconnected processes, revealing metabolic strategies that minimize ATP losses as emergent properties of the system rather than being predefined *a priori*. Our experimental results aligned well with the model's predictions, indicating that cFBA model successfully captured the key features of substrate interactions and energy flows. The strong agreement between model predictions and experimental results underscores the power of metabolic modelling, particularly cFBA, in dissecting complex metabolic behaviours in dynamic microbial ecosystems.

In this research we provide experimental evidence of a positive reciprocal synergistic interaction between acetate and aspartate. Similar experimental evidence further validating this type of interaction has been observed for the concurrent uptake of acetate with aspartate (Qiu et al., 2019), succinate and fumarate (Chen et al., 2023). In addition, research on the concurrent uptake of acetate and aspartate support our concept of a non-synergetic relation between the two substrates due to their similar metabolic requirements. Our model could not detect any co-substrate combinations with acetate that would lower biomass yields (in essence, negative interactions). This limitation stems from the model's focus on global biomass yield optimization. Potential negative interactions might arise when dealing with substrates that activate stress responses (Blank et al., 2008) or an overproduction of reductive potential (Chen and Wu, 2022, Cape et al., 2009) and warrant further investigation. Additionally, further validation of these mechanisms could involve experiments with isotopically labelled substrates (*e.g.*, ^{13}C-acetate), though such quantitative approaches applied to biofilms and microbial communities still require methodological development and standardization. More broadly, our findings reinforce the fundamental advantages of co-substrate metabolism (Liu et al., 2020), which have been classified into several key benefits: (i) improved balance of biosynthetic precursors, (ii) simultaneous activation of multiple metabolic pathways for enhanced carbon conversion, (iii) metabolic shortcuts that bypass regulatory bottlenecks, and (iv) the ability to decouple growth from lag-phase constraints. In our system, these benefits manifest through reciprocal metabolic synergy, where acetate and aspartate co-utilisation reduces ATP losses, enhances redox stability, and improves growth efficiency. In wastewater treatment plants, PAO species belonging to the genus *Tetrasphaera* and *Azonexus* have also been reported. Future research is warranted on how co-substrate utilisation can influence their metabolism. This mirrors findings in other microbial systems, where synergistic co-substrate feeding enhances biosynthesis, such as lipid production in yeast and microalgae or mixotrophic fermentations to derive net-negative CO_2 processes (Park et al., 2019). These results highlight that the principles governing co-substrate utilization in PAOs extend beyond wastewater treatment, providing a generalizable framework for understanding microbial metabolic interactions in soils, aquatic ecosystems, and biotechnological applications. Future studies should explore how metabolic flexibility shapes microbial competition and community assembly in natural environments, ultimately influencing ecosystem stability and nutrient cycling at broader scales.

5. Conclusions

- Co-utilisation of acetate and aspartate by "*Ca.* Accumulibacter" results in synergistic metabolic interactions that improve biomass yield and reduce ATP losses.
- Acetate conversion to PHA benefits from NADH generated during aspartate uptake, while aspartate uptake is supported by acetyl-CoA produced from acetate uptake.
- Glycogen cycling related to growth on acetate is energy demanding, co-utilisation of another substrates (*e.g.*, aspartate, succinate, fumarate) derives a source of NADH generation, thereby reducing the dependence on glycogen cycling.
- A holistic consideration of the entire EBPR cycle is essential to fully understand the metabolic strategies and optimize the performance of PAOs.
- Synergistic interactions arising from metabolic optimization present an opportunity for co-utilization of carbon substrates that can be exploited to enhance the yield of bio-based processes.

CRediT authorship contribution statement

Timothy Páez-Watson: Writing – review & editing, Writing – original draft, Visualization, Methodology, Investigation, Formal analysis. **Casper Jansens:** Writing – original draft, Visualization, Methodology, Investigation, Formal analysis. **Mark C.M. van Loosdrecht:** Writing – review & editing, Writing – original draft, Supervision, Methodology, Funding acquisition, Formal analysis, Conceptualization. **Samarpita Roy:** Writing – review & editing, Writing – original draft, Visualization, Supervision, Software, Project administration, Methodology, Investigation, Funding acquisition, Data curation, Conceptualization.

Declaration of competing interest

The authors declare that they have no known competing financial interests or personal relationships that could have appeared to influence the work reported in this paper.

Acknowledgements

SR was supported by the European Union's Horizon Europe research and innovation program under the Marie Skłodowska-Curie grant agreement No 101068900. **MvL, SR** and **TPW** were supported by the SIAM Gravitation Grant 024.002.002, The Netherlands Organization for Scientific Research.

Supplementary materials

Supplementary material associated with this article can be found, in the online version, at doi:10.1016/j.watres.2025.124401.

Data availability

SBML models, files and results available at https://github.com/TP-Watson/PAOs_co-substrates_cFBA. Sequencing data deposited under BioProject no. PRJNA1191880, BioSample accession no. SAMN45106973.

References

Adolfsen, K.J., Brynildsen, M.P., 2015. Futile cycling increases sensitivity toward oxidative stress in *Escherichia coli*. Metab. Eng. 29, 26–35.

Amann, R.I., Binder, B.J., Olson, R.J., Chisholm, S.W., Devereux, R., Stahl, D., 1990. Combination of 16S rRNA-targeted oligonucleotide probes with flow cytometry for analyzing mixed microbial populations. Appl. Environ. Microbiol. 56 (6), 1919–1925.

Andrews, S. FastQC: a Quality Control Tool for High Throughput Sequence Data. Cambridge, United Kingdom: 2010.
Bengtsson, S., Hallquist, J., Werker, A., Welander, T., 2008. Acidogenic fermentation of industrial wastewaters: effects of chemostat retention time and pH on volatile fatty acids production. Biochem. Eng. J. 40 (3), 492–499.
Blank, L.M., Ionidis, G., Ebert, B.E., Bühler, B., Schmid, A., 2008. Metabolic response of Pseudomonas putida during redox biocatalysis in the presence of a second octanol phase. FEBS. J. 275 (20), 5173–5190.
Brdjanovic, D., Van Loosdrecht, M., Hooijmans, C., Mino, T., Alaerts, G., Heijnen, J., 1998. Effect of polyphosphate limitation on the anaerobic metabolism of phosphorus-accumulating microorganisms. Appl. Microbiol. Biotechnol. 50 (2), 273–276.
Brdjanovic, D., van Loosdrecht, M.C., Hooijmans, C.M., Mino, T., Alaerts, G.J., Heijnen, J.J., 1998. Bioassay for glycogen determination in biological phosphorus removal systems. Water Sci. Technol. 37 (4–5), 541–547.
Cape, J.L., Aidasani, D., Kramer, D.M., Bowman, M.K., 2009. Substrate redox potential controls superoxide production kinetics in the cytochrome bc complex. Biochemistry 48 (45), 10716–10723.
Carvalheira, M., Oehmen, A., Carvalho, G., Reis, M.A.M., 2014. The effect of substrate competition on the metabolism of polyphosphate accumulating organisms (PAOs). Water. Res. 64, 149–159. https://doi.org/10.1016/j.watres.2014.07.004.
Chaumeil, P.-A., Mussig, A.J., Hugenholtz, P., Parks, D.H., 2022. GTDB-Tk v2: memory friendly classification with the genome taxonomy database. Bioinformatics. 38 (23), 5315–5316. https://doi.org/10.1093/bioinformatics/btac672 acccessed 10/28/2024.
Chen, W.-Y., Wu, J.-H., 2022. Microbiome composition resulting from different substrates influences trichloroethene dechlorination performance. J. Environ. Manage 303, 114145.
Chen, L., Wei, G., Zhang, Y., Wang, K., Wang, C., Deng, X., Li, Y., Xie, X., Chen, J., Huang, F., 2023. Candidatus Accumulibacter use fermentation products for enhanced biological phosphorus removal. Water. Res. 246, 120713.
Chen, S., 2023. Ultrafast one-pass FASTQ data preprocessing, quality control, and deduplication using fastp. Imeta 2 (2), e107.
Chitraju, C., Mejhert, N., Haas, J.T., Diaz-Ramirez, L.G., Grueter, C.A., Imbriglio, J.E., Pinto, S., Koliwad, S.K., Walther, T.C., Farese, R.V., 2017. Triglyceride synthesis by DGAT1 protects adipocytes from lipid-induced ER stress during lipolysis. Cell Metab. 26 (2), 407–418.e403.
da Silva, L.G., Gamez, K.O., Gomes, J.C., Akkermans, K., Welles, L., Abbas, B., van Loosdrecht, M.C., Wahl, S.A., 2020. Revealing the Metabolic Flexibility of "Candidatus Accumulibacter phosphatis" through Redox Cofactor Analysis and Metabolic Network Modeling. Appl. Environ. Microbiol. 86 (24).
Daims, H., Brühl, A., Amann, R., Schleifer, K.-H., Wagner, M., 1999. The domain-specific probe EUB338 is insufficient for the detection of all Bacteria: development and evaluation of a more comprehensive probe set. Syst. Appl. Microbiol. 22 (3), 434–444.
Daims, H., Lücker, S., Wagner, M., 2006. Daime, a novel image analysis program for microbial ecology and biofilm research. Environ. Microbiol. 8 (2), 200–213.
Edgar, R.C., 2004. MUSCLE: a multiple sequence alignment method with reduced time and space complexity. BMC. Bioinformatics. 5, 1–19.
Egli, T., Lendenmann, U., Snozzi, M., 1993. Kinetics of microbial growth with mixtures of carbon sources. Antonie Van Leeuwenhoek 63 (3), 289–298.
Elahinik, A., Li, L., Pabst, M., Abbas, B., Xevgenos, D., van Loosdrecht, M.C., Pronk, M., 2023. Aerobic granular sludge phosphate removal using glucose. Water. Res. 247, 120776.
García Martín, H., Ivanova, N., Kunin, V., Warnecke, F., Barry, K.W., McHardy, A.C., Yeates, C., He, S., Salamov, A.A., Szeto, E., et al., 2006. Metagenomic analysis of two enhanced biological phosphorus removal (EBPR) sludge communities. Nat. Biotechnol. 24 (10), 1263–1269. https://doi.org/10.1038/nbt1247 From NLM.
Gebremariam, S.Y., Beutel, M.W., Christian, D., Hess, T.F., 2012. Effects of glucose on the performance of enhanced biological phosphorus removal activated sludge enriched with acetate. Bioresour. Technol. 121, 19–24.
Gommers, P., Van Schie, B., Van Dijken, J., Kuenen, J., 1988. Biochemical limits to microbial growth yields: an analysis of mixed substrate utilization. Biotechnol. Bioeng. 32 (1), 86–94.
Huang, M.-h., Li, Y.-m., Gu, G.-w., 2010. Chemical composition of organic matters in domestic wastewater. Desalination. 262 (1–3), 36–42.
Johnson, L.S., Eddy, S.R., Portugaly, E., 2010. Hidden Markov model speed heuristic and iterative HMM search procedure. BMC. Bioinformatics. 11, 1–8.
Kang, D.D., Li, F., Kirton, E., Thomas, A., Egan, R., An, H., Wang, Z., 2019. MetaBAT 2: an adaptive binning algorithm for robust and efficient genome reconstruction from metagenome assemblies. PeerJ. 7, e7359.
Kleikamp, H.B., Grouzdev, D., Schaasberg, P., van Valderen, R., van der Zwaan, R., van de Wijgaart, R., Lin, Y., Abbas, B., Pronk, M., van Loosdrecht, M.C., 2022. Comparative metaproteomics demonstrates different views on the complex granular sludge microbiome. bioRxiv. 2022.2003. 2007.483319.
Kleikamp, H.B., Grouzdev, D., Schaasberg, P., van Valderen, R., van der Zwaan, R., van de Wijgaart, R., Lin, Y., Abbas, B., Pronk, M., van Loosdrecht, M.C.M., 2023. metagenomics and 16S rRNA sequencing provide different perspectives on the aerobic granular sludge microbiome. Water. Res. 246, 120700.
Kong, Y., Nielsen, J.L., Nielsen, P.H., 2004. Microautoradiographic study of Rhodocyclus-related polyphosphate-accumulating bacteria in full-scale enhanced biological phosphorus removal plants. Appl. Environ. Microbiol. 70 (9), 5383–5390.
Kortstee, G.J., Appeldoorn, K.J., Bonting, C.F., van Niel, E.W., van Veen, H.W., 1994. Biology of polyphosphate-accumulating bacteria involved in enhanced biological phosphorus removal. FEMS Microbiol. Rev. 15 (2–3), 137–153.
Kozlov, A.M., Darriba, D., Flouri, T., Morel, B., Stamatakis, A., 2019. RAxML-NG: a fast, scalable and user-friendly tool for maximum likelihood phylogenetic inference. Bioinformatics. 35 (21), 4453–4455.
Letunic, I., Bork, P., 2024. Interactive Tree of Life (iTOL) v6: recent updates to the phylogenetic tree display and annotation tool. Nucleic. Acids. Res. gkae268.
Liu, L., Bockmayr, A., 2020. Regulatory dynamic enzyme-cost flux balance analysis: a unifying framework for constraint-based modeling. J. Theor. Biol. 501, 110317.
Liu, N., Santala, S., Stephanopoulos, G., 2020. Mixed carbon substrates: a necessary nuisance or a missed opportunity? Curr. Opin. Biotechnol. 62, 15–21.
Lu, H., Oehmen, A., Virdis, B., Keller, J., Yuan, Z., 2006. Obtaining highly enriched cultures of Candidatus Accumulibacter phosphates through alternating carbon sources. Water. Res. 40 (20), 3838–3848.
Mahadevan, R., Edwards, J.S., Doyle III, F.J., 2002. Dynamic flux balance analysis of diauxic growth in *Escherichia coli*. Biophys. J. 83 (3), 1331–1340.
McIlroy, S.J., Starnawska, A., Starnawski, P., Saunders, A.M., Nierychlo, M., Nielsen, P. H., Nielsen, J.L., 2016. Identification of active denitrifiers in full-scale nutrient removal wastewater treatment systems. Environ. Microbiol. 18 (1), 50–64.
Mino, T., Arun, V., Tsuzuki, Y., Matsuo, T., 1987. Effect of phosphorus accumulation on acetate metabolism in the biological phosphorus removal process. Biological Phosphate Removal from Wastewaters. Elsevier, pp. 27–38.
Mino, T., Van Loosdrecht, M., Heijnen, J., 1998. Microbiology and biochemistry of the enhanced biological phosphate removal process. Water. Res. 32 (11), 3193–3207.
Nguyen, H.T.T., Kristiansen, R., Vestergaard, M., Wimmer, R., Nielsen, P.H., 2015. Intracellular accumulation of glycine in polyphosphate-accumulating organisms in activated sludge, a novel storage mechanism under dynamic anaerobic-aerobic conditions. Appl. Environ. Microbiol. 81 (14), 4809–4818.
Nielsen, J., 2017. Systems biology of metabolism. Annu. Rev. Biochem. 86 (1), 245–275.
Nurk, S., Meleshko, D., Korobeynikov, A., Pevzner, P.A., 2017. metaSPAdes: a new versatile metagenomic assembler. Genome Res. 27 (5), 824–834.
Oehmen, A., Zeng, R.J., Keller, J., Yuan, Z., 2007. Modeling the Aerobic Metabolism of Polyphosphate-Accumulating Organisms Enriched with Propionate as a Carbon Source. Water Environ. Res. 79 (13), 2477–2486.
Oehmen, A., Lemos, P.C., Carvalho, G., Yuan, Z., Keller, J., Blackall, L.L., Reis, M.A.M., 2007. Advances in enhanced biological phosphorus removal: from micro to macro scale. Water. Res. 41 (11), 2271–2300. https://doi.org/10.1016/j.watres.2007.02.030.
Oehmen, A., Carvalho, G., Lopez-Vazquez, C., Van Loosdrecht, M., Reis, M., 2010. Incorporating microbial ecology into the metabolic modelling of polyphosphate accumulating organisms and glycogen accumulating organisms. Water. Res. 44 (17), 4992–5004.
Onnis-Hayden, A., Majed, N., Li, Y., Rahman, S.M., Drury, D., Risso, L., Gu, A.Z., 2020. Impact of solid residence time (SRT) on functionally relevant microbial populations and performance in full-scale enhanced biological phosphorus removal (EBPR) systems. Water Environ. Res. 92 (3), 389–402.
Orth, J.D., Thiele, I., Palsson, B.Ø., 2010. What is flux balance analysis? Nat. Biotechnol. 28 (3), 245–248.
Oyserman, B.O., Noguera, D.R., del Rio, T.G., Tringe, S.G., McMahon, K.D., 2016. Metatranscriptomic insights on gene expression and regulatory controls in *Candidatus* Accumulibacter phosphatis. ISMe J. 10 (4), 810–822.
Páez-Watson, T., van Loosdrecht, M.C., Wahl, S.A., 2023. Predicting the impact of temperature on metabolic fluxes using resource allocation modelling: application to polyphosphate accumulating organisms. Water. Res. 228, 119365.
Páez-Watson, T., Tomás-Martínez, S., de Wit, R., Keisham, S., Tateno, H., van Loosdrecht, M.C., Lin, Y., 2024. Sweet Secrets: exploring Novel Glycans and Glycoconjugates in the Extracellular Polymeric Substances of "Candidatus Accumulibacter. ACS. ES. T. Water. 4 (8), 3391–3399.
Páez-Watson, T., Hernández Medina, R., Vellekoop, L., van Loosdrecht, M.C., Wahl, S.A., 2024. Conditional Flux Balance Analysis (cFBA) Toolbox for python: application to research metabolism in cyclic environments. Bioinform. Adv. vbae174.
Páez-Watson, T., van Loosdrecht, M.C., Wahl, S.A., 2024. From metagenomes to metabolism: systematically assessing the metabolic flux feasibilities for "*Candidatus* Accumulibacter" species during anaerobic substrate uptake. Water. Res. 250, 121028.
Park, J.O., Liu, N., Holinski, K.M., Emerson, D.F., Qiao, K., Woolston, B.M., Xu, J., Lazar, Z., Islam, M.A., Vidoudez, C., 2019. Synergistic substrate cofeeding stimulates reductive metabolism. Nat. Metab. 1 (6), 643–651.
Parks, D.H., Imelfort, M., Skennerton, C.T., Hugenholtz, P., Tyson, G.W., 2015. CheckM: assessing the quality of microbial genomes recovered from isolates, single cells, and metagenomes. Genome Res. 25 (7), 1043–1055.
Petriglieri, F., Singleton, C., Peces, M., Petersen, J.F., Nierychlo, M., Nielsen, P.H., 2021. Candidatus Dechloromonas phosphoritropha" and "*Ca.* D. phosphorivorans", novel polyphosphate accumulating organisms abundant in wastewater treatment systems. ISMe J. 15 (12), 3605–3614.
Petriglieri, F., Singleton, C.M., Kondrotaite, Z., Dueholm, M.K., McDaniel, E.A., McMahon, K.D., Nielsen, P.H., 2022. Reevaluation of the Phylogenetic Diversity and Global Distribution of the Genus "Candidatus Accumulibacter". mSystems. 7 (3), e00016–e00022.
Pijuan, M., Saunders, A.M., Guisasola, A., Baeza, J.A., Casas, C., Blackall, L., 2004. Enhanced biological phosphorus removal in a sequencing batch reactor using propionate as the sole carbon source. Biotechnol. Bioeng. 85 (1), 56–67.
Qiu, G., Zuniga-Montanez, R., Law, Y., Thi, S.S., Nguyen, T.Q.N., Eganathan, K., Liu, X., Nielsen, P.H., Williams, R.B., Wuertz, S., 2019. Polyphosphate-accumulating organisms in full-scale tropical wastewater treatment plants use diverse carbon sources. Water. Res. 149, 496–510.
Qiu, G., Liu, X., Saw, N.M.M.T., Law, Y., Zuniga-Montanez, R., Thi, S.S., Ngoc Nguyen, T. Q., Nielsen, P.H., Williams, R.B., Wuertz, S., 2019. Metabolic traits of Candidatus

Accumulibacter clade IIF strain SCELSE-1 using amino acids as carbon sources for enhanced biological phosphorus removal. Environ. Sci. Technol. 54 (4), 2448–2458.
Rügen, M., Bockmayr, A., Steuer, R., 2015. Elucidating temporal resource allocation and diurnal dynamics in phototrophic metabolism using conditional FBA. Sci. Rep. 5, 15247.
Reimers, A.-M., Knoop, H., Bockmayr, A., Steuer, R., 2017. Cellular trade-offs and optimal resource allocation during cyanobacterial diurnal growth. Proceed. National Acad. Sci. 114 (31), E6457–E6465.
Rodrigo, M., Seco, A., Ferrer, J., Penya-Roja, J., 1999. The effect of sludge age on the deterioration of the enhanced biological phosphorus removal process. Environ. Technol. 20 (10), 1055–1063.
Roy, S., Guanglei, Q., Zuniga-Montanez, R., Williams, R.B., Wuertz, S., 2021. Recent advances in understanding the ecophysiology of enhanced biological phosphorus removal. Curr. Opin. Biotechnol. 67, 166–174.
Rubio-Rincón, F.J., Welles, L., Lopez-Vazquez, C.M., Abbas, B., van Loosdrecht, M.C., Brdjanovic, D., 2019. Effect of lactate on the microbial community and process performance of an EBPR system. Front. Microbiol. 10, 125.
Sarkar, D., Mueller, T.J., Liu, D., Pakrasi, H.B., Maranas, C.D., 2019. A diurnal flux balance model of Synechocystis sp. PCC 6803 metabolism. PLoS. Comput. Biol. 15 (1), e1006692.
Sharma, A.K., Wolfrum, C., 2023. Lipid cycling isn't all futile. Nat. Metab. 5 (4), 540–541.
Sharma, A.K., Khandelwal, R., Wolfrum, C., 2024. Futile cycles: emerging utility from apparent futility. Cell Metab.
Skennerton, C.T., Barr, J.J., Slater, F.R., Bond, P.L., Tyson, G.W., 2015. Expanding our view of genomic diversity in CandidatusAccumulibacter clades. Environ. Microbiol. 17 (5), 1574–1585. https://doi.org/10.1111/1462-2920.12582. From NLM.
Smolders, G., Van der Meij, J., Van Loosdrecht, M., Heijnen, J., 1994. Model of the anaerobic metabolism of the biological phosphorus removal process: stoichiometry and pH influence. Biotechnol. Bioeng. 43 (6), 461–470.
Smolders, G., Van der Meij, J., Van Loosdrecht, M., Heijnen, J., 1994. Stoichiometric model of the aerobic metabolism of the biological phosphorus removal process. Biotechnol. Bioeng. 44 (7), 837–848.
Smolders, G., Van der Meij, J., Van Loosdrecht, M., Heijnen, J., 1995. A structured metabolic model for anaerobic and aerobic stoichiometry and kinetics of the biological phosphorus removal process. Biotechnol. Bioeng. 47 (3), 277–287.
Toja Ortega, S., Pronk, M., de Kreuk, M.K., 2021. Anaerobic hydrolysis of complex substrates in full-scale aerobic granular sludge: enzymatic activity determined in different sludge fractions. Appl. Microbiol. Biotechnol. 105 (14), 6073–6086.
Van Loosdrecht, M., Smolders, G., Kuba, T., Heijnen, J., 1997. Metabolism of micro-organisms responsible for enhanced biological phosphorus removal from wastewater, Use of dynamic enrichment cultures. Antonie Van Leeuwenhoek 71 (1–2), 109–116.
Welles, L., Tian, W., Saad, S., Abbas, B., Lopez-Vazquez, C., Hooijmans, C., Van Loosdrecht, M., Brdjanovic, D., 2015. Accumulibacter clades Type I and II performing kinetically different glycogen-accumulating organisms metabolisms for anaerobic substrate uptake. Water. Res. 83, 354–366.
Whang, L.M., Park, J.K., 2006. Competition between polyphosphate-and glycogen-accumulating organisms in enhanced-biological-phosphorus-removal systems: effect of temperature and sludge age. Water Environ. Res. 78 (1), 4–11.
Whitton, B.A., 2012. Ecology of Cyanobacteria II: Their Diversity in Space and Time. Springer Science & Business Media.
Winkler, M.-K., Bassin, J., Kleerebezem, R., De Bruin, L., Van den Brand, T., Van Loosdrecht, M., 2011. Selective sludge removal in a segregated aerobic granular biomass system as a strategy to control PAO–GAO competition at high temperatures. Water. Res. 45 (11), 3291–3299.
Wollmuth, E.M., Angert, E.R., 2023. Microbial circadian clocks: host-microbe interplay in diel cycles. BMC. Microbiol. 23 (1), 124.
Wood, D.E., Lu, J., Langmead, B., 2019. Improved metagenomic analysis with Kraken 2. Genome Biol. 20, 1–13.
Wu, W., Dijkstra, P., Hungate, B.A., Shi, L., Dippold, M.A., 2022. *In situ* diversity of metabolism and carbon use efficiency among soil bacteria. Sci. Adv. 8 (44), eabq3958.
Yuan, Q., Sparling, R., Lagasse, P., Lee, Y., Taniguchi, D., Oleszkiewicz, J., 2010. Enhancing biological phosphorus removal with glycerol. Water Sci. Technol. 61 (7), 1837–1843.
Zhang, Y., Li, C., Li, H., Song, Y., Zhao, Y., Zhai, L., Wang, H., Zhong, R., Tang, H., Zhu, D., 2016. miR-378 activates the pyruvate-PEP futile cycle and enhances lipolysis to ameliorate obesity in mice. EBioMedicine 5, 93–104.
Ziliani, A., Bovio-Winkler, P., Cabezas, A., Etchebehere, C., Garcia, H.A., López-Vázquez, C.M., Brdjanovic, D., van Loosdrecht, M.C., Rubio-Rincón, F.J., 2023. Putative metabolism of *Ca.* Accumulibacter via the utilization of glucose. Water. Res. 229, 119446.